

Neutrino Whispers from Dark Stars Seeding Supermassive Black Holes

Thomas Schwemberger^{1,*} and Volodymyr Takhistov^{2,3,4,5,†}

¹*Department of Physics and Institute for Fundamental Science, University of Oregon, Eugene, OR 97403, USA*

²*International Center for Quantum-field Measurement Systems for Studies of the Universe and Particles (QUP, WPI), High Energy Accelerator Research Organization (KEK), Oho 1-1, Tsukuba, Ibaraki 305-0801, Japan*

³*Theory Center, Institute of Particle and Nuclear Studies (IPNS), High Energy Accelerator Research Organization (KEK), Tsukuba 305-0801, Japan*

⁴*Graduate University for Advanced Studies (SOKENDAI), 1-1 Oho, Tsukuba, Ibaraki 305-0801, Japan*

⁵*Kavli Institute for the Physics and Mathematics of the Universe (WPI), The University of Tokyo Institutes for Advanced Study, The University of Tokyo, Kashiwa, Chiba 277-8583, Japan*

First stars powered by dark matter (DM) heating instead of fusion can appear in the early Universe from theories of new physics. These dark stars (DSs) can be significantly larger and cooler than early Population III stars, and could seed supermassive black holes (SMBHs). We show that neutrino emission from supermassive DSs provides a novel window into probing SMBH progenitors. We estimate first DS constraints using data from Super-Kamiokande and IceCube neutrino experiments, and consistent with James Webb Space Telescope observations. Upcoming neutrino telescopes offer distinct opportunities to further explore DS properties.

Introduction.— The first generation stars are thought to have played a pivotal role in the Universe, including shaping cosmic evolution, influencing reionization and chemical enrichment. These population III (Pop III) zero-metallicity stars are believed to have formed from the gravitational collapse of pristine gas left over after the Big Bang, within dark matter (DM) mini-halos of mass $\sim 10^5 - 10^7 M_\odot$ around redshifts $z \sim 20$ (e.g. [1–3]). Despite their significance, Pop III stars are yet to be observed, although candidates have been suggested [4–6].

Supermassive black holes (SMBHs) with masses ranging $\sim 10^6 - 10^9 M_\odot$ are ubiquitous at the centers of galaxies, powering quasars and active galactic nuclei (AGN). The origin of SMBHs at high redshifts remains a mystery, especially in light of recent observations by the James Webb Space Telescope (JWST) [7–10] suggesting SMBH detections even at redshifts of up to $z \simeq 10.3$ [11]. Achieving the necessary rapid growth of such massive objects challenges Eddington-limited accretion and hierarchical mergers of stellar-mass black holes on relevant cosmological timescales (e.g. [12, 13]). While Pop III stars offer plausible candidates for forming lighter $\sim 10^2 - 10^3 M_\odot$ SMBH seeds, alternative scenarios such as direct collapse have also been suggested (see e.g. [14, 15] for review) and further investigation is necessary.

An intriguing distinct class of first stars, known as dark stars (DSs), powered by heating from DM constituting a small fraction of their mass instead of fusion, has been put forth and that could seed SMBHs [16–18]. DM heating can be a general byproduct of annihilation of weakly interacting massive particles (WIMPs) [16], but can also arise in contexts such as self-interacting DM [19]. During formation, the contraction of baryonic matter induces adiabatic contraction of DM, leading to high DM densities sufficient for efficient annihilation. The energy re-

leased from DM annihilation halts the collapse at low temperatures, preventing the onset of nuclear fusion. When the DM fuel is exhausted, the DS collapses into a black hole. Massive DSs seeding SMBHs could also explain paucity of intermediate-mass black holes [20]. Although detection of DS is challenging, their electromagnetic emission contributing to photon background has been considered [21–23]. Recently, it has been suggested that some high-redshift galaxy candidates observed by JWST could be spectroscopic manifestations of DSs [24].

In this work we investigate neutrino signatures originating from DSs and establish a new observational window into the progenitors of SMBHs. Going beyond previous limited considerations [21, 25], we show that DSs can produce detectable neutrino signals and we set constraints on DM annihilation using data from neutrino experiments. Furthermore, we show that our findings are consistent with observations from the JWST. Our study bridges key gaps between other directions, such as neutrino signatures [26–29] from intermediate supermassive stars that might arise from star cluster collapse or primordial clouds in astrophysical SMBH formation paths.

Dark star population.— The DS population is expected to trace that of the first DM halos. The comoving number density distribution of DM halos based on a generalized halo mass function can be expressed as

$$\frac{dn_h}{dM_h} = \frac{\rho_m}{M_h} \sqrt{\frac{2A^2\beta}{\pi}} \left(1 + (\beta\nu^2)^{-p}\right) e^{-\beta\nu^2/2} \frac{d\nu}{dM_h}, \quad (1)$$

where $\nu = \delta_c/D(z)\sigma(M_h)$ with $D(z) = \delta(a)/\delta(1)$ being the linear growth factor [30], $a = (1+z)^{-1}$ being the scale factor, and δ as defined in Ref. [31]. Here, $\delta_c = 1.68$ is the critical overdensity above which a spherically symmetric perturbation region will collapse to form virialized halo. $\rho_m = \rho_c\Omega_m(1+z)^3$ is the average mass density of the Uni-

verse scaled to critical density $\rho_c = 9 \times 10^{-30} \text{ g cm}^{-3}$ at present by fraction $\Omega_m = 0.3$ [32]. In Eq. (1) parameters $(A, \beta, p) = (0.5, 1, 0)$ correspond to the Press-Schechter mass function [33], which we focus on throughout. We find similar results for the Sheth-Tormen [34] mass function, corresponding to $(A, \beta, p) = (0.322, 0.707, 0.3)$. The variance of the initial density fluctuation field $\sigma(M_h)$ is

$$\sigma^2(M_h) = \frac{1}{2\pi^2} \int W^2(kR_{M_h}) P_\delta(k) k^2 dk \quad (2)$$

where $W(x) = 3(\sin x - x \cos x)/x^3$ is a top-hat window function smoothing density fluctuation over scale $R_{M_h} = (3M_h/4\pi\rho_m)$. This is derived from the matter power spectrum $P_\delta(k) = A_s(k \text{ Mpc})^{n_s} T^2(k)$ where A_s is normalized by σ_8 [35] and $T(k)$ is transfer function fitted to cold DM model [36] with a spectral index $n_s = 0.965$ [32].

We model the DS formation rate to be proportional to the halo formation rate $d^2n_h/dM_h dt$ up to a scaling f_{SMDS} that quantifies the fraction of DM halos hosting DSs. We do not consider the possible dependence of f_{SMDS} on halo mass and redshift and assume minimal delay between halo formation and the DS formation of initial mass $M_{\text{DS},i} \simeq 5 M_\odot$, which doesn't significantly affect our results unless these timescales are comparable to the DS lifetime. The DS growth proceeds by accretion, and we consider that halo mass does not appreciably change during this period. We have confirmed that our DS luminosity as a function of mass matches numerically computed 1D stellar evolution of DS results of Ref. [37] within a factor of few, assuming a constant accretion rate of $\dot{M}_{\text{DS}} = 10^{-9} M_h \text{ yr}^{-1}$ with DS mass following $M_{\text{DS}}(t) = M_{\text{DS},i} + \dot{M}_{\text{DS}} t$.

The comoving number density of DSs surviving to a redshift z at a given cosmological time t in halos of mass M_h and age τ is given by

$$\frac{dn_{\text{DS}}}{dM_h} = f_{\text{SMDS}} \int_{z(t)}^{\infty} dz' \left| \frac{dt}{dz'} \right| \frac{d^2n_h}{dt dM_h}(M_h, z'(t - \tau)) \quad (3)$$

where we consider $M_{\text{DS}}^{\text{lim}} = 10^{-2} M_h$ as the upper limit of DS mass. Here $dz/dt = (1+z)H(z)$ with the Hubble parameter for Λ CDM $H(z) \simeq H_0 \sqrt{\Omega_m(1+z)^3 + \Omega_\Lambda}$, where $H_0 = 67.4 \text{ km/s/Mpc}$ is the Hubble constant at present, $\Omega_\Lambda = 0.7$ accounts for dark energy density and the radiation density of the Universe is neglected.

The total DS number n_{DS} can then be obtained by integrating Eq. (3) over the halos with DSs. For the lower limit we take $M_{h,\text{min}} \sim 10^6 M_\odot$ as the minimum mass where molecular hydrogen cooling causes protostellar clouds to collapse [38]. If lighter halos $M_h \sim 10^5 M_\odot$ allow for DSs, this could significantly enhance their abundance (see Supplemental Material). However, we estimate that the lighter and less-luminous DSs would only contribute a factor ~ 2 enhancement to the total resulting neutrino flux. For the upper halo mass limit we take

$M_{h,\text{max}} \sim 10^9 M_\odot$, but our results are not very sensitive to this limit as such massive halos are rare at $z \gtrsim 15$.

The exact lifetimes and upper mass limits of DSs require further exploration. A large upper limit on DS mass being $\sim 5\%$ of the halo mass was considered in Ref. [38]. Recent high redshift SMBH observations appear to favor SMBH formation from $\sim 10^5 M_\odot$ "heavy seeds" at $z \gtrsim 15$ [11]. Considering halos of mass $M_h > 10^6 M_\odot$ as the supermassive DS hosts, the average halo mass is around $\sim 10^7 M_\odot$. Typical DS masses of $\sim 10^5 M_\odot$ can be achieved considering DSs grow to $\sim 1\%$ of host halo mass. Our results can be readily rescaled to account for different DS masses by appropriately considering the DM cross-section in Eq. (4). Smaller DSs are more challenging to detect with telescopes, with weakened constraints and allowing for higher abundance at lower redshifts.

Considering DS formation in mini-halos at redshifts $z \gtrsim 25$ and that they undergo collapse by $z \simeq 15$, as discussed below, the corresponding DS lifetime is $\mathcal{O}(10^8)$ yrs. Such DSs powered to luminosities of $\sim 10^{10} L_\odot$ will require fueling of $\sim 10^6 M_\odot$ of DM, roughly percent-level of typical halo masses. DSs consuming heavier DM have smaller luminosities and can be expected to deplete host halos less significantly (see e.g. Ref. [39] discussion).

Dark star emission.— As baryonic matter undergoes protostellar collapse, it deepens the gravitational potential well at the center of a DM mini-halo of mass M_h . This alters the orbits of dissipation-less DM particles in accordance with the adiabatic invariant [40], $rM(r) = \text{const.}$, where $M(r)$ is the mass enclosed within radius r . As $M(r)$ increases due to baryonic inflow, r must decrease, leading to the adiabatic contraction of DM. This process concentrates DM at the center of the halo, where it can reach sufficiently high densities for efficient annihilation [16]. The energy released by DM annihilation heats the surrounding baryonic gas, stalling further collapse. The additional energy source in stellar evolution results in formation of a new DS category of early stars with much lower densities and temperatures.

We compute DS luminosity evolution considering an analytic polytropic model, as described in detail in Supplementary Materials. The resulting luminosity for DS of mass M_{DS} can be well fit by

$$L_{\text{DS}} \simeq 2.1 \times 10^4 \left(\frac{M_{\text{DS}}(t)}{M_\odot} \right)^{0.85} \left(\frac{\langle \sigma v \rangle}{10^{-26} \text{ cm}^2/\text{s}} \right)^{0.45} \times \left(\frac{m_\chi(1 - f_\nu)}{100 \text{ GeV}} \right)^{-0.46} L_\odot \quad (4)$$

where reference $\langle \sigma v \rangle \simeq 10^{-26} \text{ cm}^3 \text{ s}^{-1}$ is the thermally averaged DM annihilation cross-section as motivated by thermal relic abundance (e.g. [41]), f_ν is the fraction of the DM mass m_χ that is converted to neutrino energy. We find approximate agreement with results of Ref. [39].

The much lower temperatures of DSs, with $\lesssim \text{few} \times 10^4 \text{ K}$ [37] at their surface, compared to Pop III stars

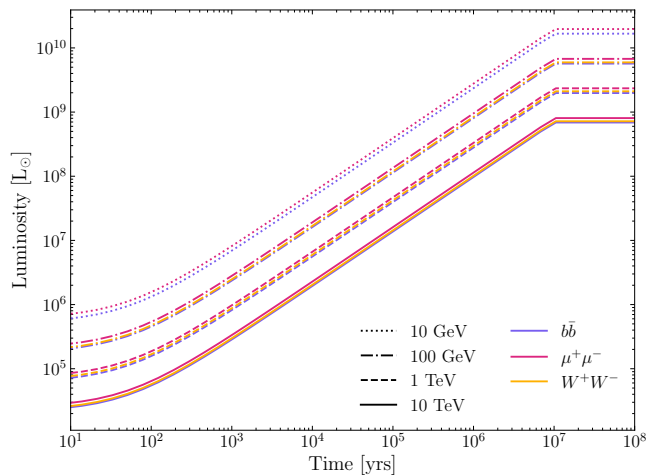


FIG. 1. Evolution of DS luminosity for different DM masses and annihilation channels. We assume baryonic accretion rate of $0.1M_{\odot} \text{ yr}^{-1}$ in a $10^8 M_{\odot}$ halo until DS reaches a mass of $\sim 10^6 M_{\odot}$. We consider that baryonic accretion stalls when DS reaches approximately $\sim 1\%$ of the host halo mass, resulting in a plateau corresponding to DS mass and luminosity being approximately constant until DM annihilation becomes inefficient and DS collapses.

result in lack of strong stellar winds. This facilitates persistent accretion of surrounding gas [42]. Depending on the mass of the host halo, DM concentration as well as baryonic accretion rates DSs can reach masses of $\sim 10^{6-7} M_{\odot}$ and luminosities of $\sim 10^{10} L_{\odot}$ [43]. In Fig. 1 we display the evolution of luminosities of DSs that grow to $\sim 10^6 M_{\odot}$ for different DM masses and annihilation channels, assuming $\dot{M}_{\text{DS}} = 0.1 M_{\odot} \text{ yr}^{-1}$ accretion rate in a $M_h = 10^8 M_{\odot}$ halo and that DM fueling persists for extended period resulting in approximately constant DS mass and luminosity once the star reaches $M_{\text{DS}} \sim 10^{-2} M_h$.

When DSs reach their maximal mass we consider efficient accretion to stall, leading to a phase of sustained stability. This persists until the surrounding DM in the host halo is sufficiently depleted, causing DM annihilation—the primary energy source of DSs—to become inefficient. At this stage, DSs collapse. High-mass DSs could collapse directly into black holes, though a brief intermediate phase of nuclear fusion is possible [43].

Supermassive black hole progenitors and JWST.— Supermassive DSs constitute intriguing possible early massive $\sim 10^{4-6} M_{\odot}$ seeds for SMBHs. We consider DS number densities consistent with distribution of SMBHs at galactic centers, one per $10^{10} M_{\odot}$ baryon mass object as can be found in some dwarf galaxies, analogous to the method of Ref. [29]. For this, we set f_{SMDS} in Eq. (3) such that number density of SMBH seeds is $n_{\text{SMBH}}(z)/(1+z)^3 \sim \rho_B/10^{10} M_{\odot}$, where $n_{\text{SMBH}}(z)$ is given by integrating Eq. (3) for contributing halos $M_h = 10^6$ to $10^9 M_{\odot}$ and $\rho_B = \rho_c \Omega_b = 4 \times 10^{-31} \text{ g/cm}^3$ is

the baryon density of the Universe with $\Omega_b = 0.0476$ [32]. We then evaluate $n_{\text{SMBH}}(z)/(1+z)^3$ just before DS collapse, taking $z = 15$ for reference, and compare with $\rho_B/10^{10} M_{\odot}$ at present. We find $f_{\text{SMDS}} \simeq 6 \times 10^{-3}$. This estimate is conservative as it does not account for such effects as mergers. To account for additional uncertainties, we consider f_{SMDS} in the range from 1% to 0.1%. Additional precision in f_{SMDS} evaluation can be obtained from detailed simulations of structure growth beyond our scope, including feedback effects [20].

Supermassive DSs could be directly detected by sensitive telescopes [24, 38, 44], providing an independent and complimentary probe. In particular, JWST’s infrared sensitivity, ability to probe the high-redshift Universe and spectroscopic tools uniquely position it to search for DSs. Recently, three supermassive DS candidates at redshifts $z \sim 11 - 14$ have been claimed from JWST Advanced Deep Extragalactic Survey (JADES) data [24]. Ref. [38] used Hubble Space Telescope (HST) data to constrain DSs up surviving to redshift $z = 10$, and showed that JWST can efficiently detect supermassive DSs up to $z = 15$ for $M_{\text{DS}} = 10^6 M_{\odot}$.

DS parameters consistent with JWST observations can be identified from the number of supermassive DSs observable in JWST at a particular redshift expressed as

$$\frac{dN_{\text{obs}}}{dz} = \frac{\theta^2}{4\pi} \int dM_{\text{DS}} f_{\text{sur}}(z, M_{\text{DS}}) f_{\text{obs}}(z, M_{\text{DS}}) \times \frac{dV_c}{dz} \frac{dn_{\text{DS}}}{dM_h}(M_h, z(t - \tau)), \quad (5)$$

where $\theta^2 = 26.4 \text{ arcmin}^2$ is the JWST coverage [52], f_{sur} and f_{obs} denote the DS fraction that survives to redshift z and the likelihood that JWST observes a DS of mass M_{DS} at redshift z respectively. Eq. (5) also includes the differential volume element dV_c/dz , with $V_c = (4\pi/3)D_M^3$ the comoving volume of the Universe where [53]

$$D_M = \left(\frac{2c}{H_0} \right) \frac{2 - \Omega_M(1-z) - (2 - \Omega_M)\sqrt{1 + z\Omega_M}}{\Omega_M^2(1+z)} \quad (6)$$

for a flat Universe without dark energy that is a good approximation at redshifts $z \gtrsim 10$ we consider. The total number of DSs observable with JWST is the integral of Eq. (5) over redshifts.

Here we consider $f_{\text{obs}}(z > 15) = 0$ and survival model f_{sur} being a step-function at $z = 15$, resulting in conservative $N_{\text{obs}} = 0$ DS candidates for all redshifts. This also maximizes possible DS neutrino flux consistent with JWST observations. In Supplemental Material we present a model of gradual DS collapse, showing that it can account for $N_{\text{obs}} \geq 1$ JWST DS candidates.

Dark star neutrino signals.— Supermassive DSs shining at high luminosities can emit significant neutrino fluxes, contributing to a diffuse background analogous to the diffuse supernova neutrino background (DSNB) in the later Universe. Unlike the DSNB produced by transient

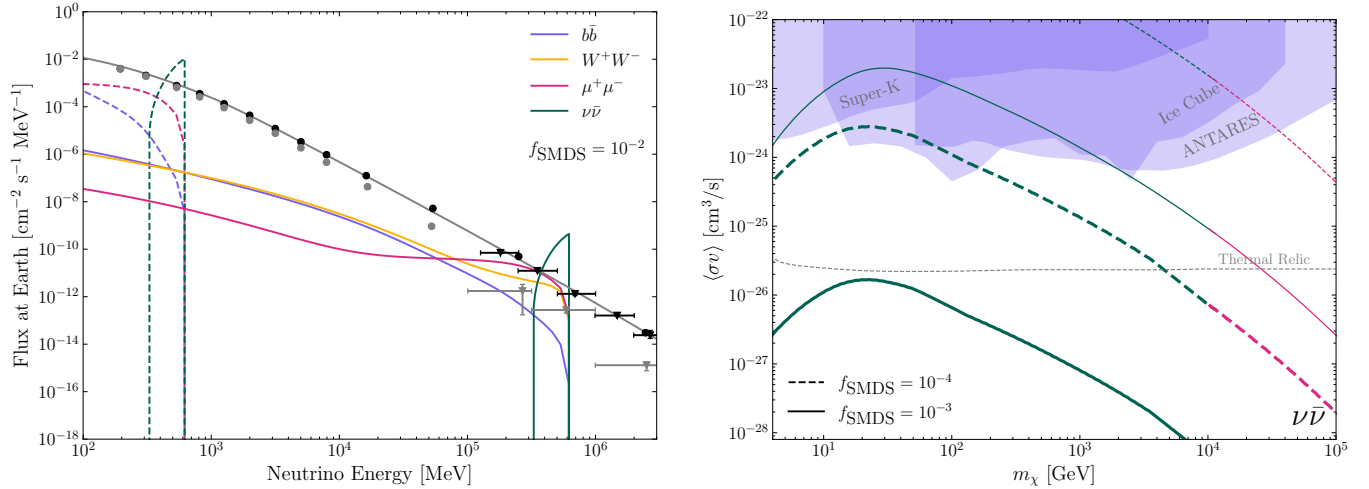


FIG. 2. [Left] The neutrino flux from $10^6 M_\odot$ supermassive DSs that can seed SMBHs for different DM annihilation channels considering DM mass $m_\chi = 10$ GeV (dashed line) and 10 TeV (solid line), for reference cross-section $\langle\sigma v\rangle = 3 \times 10^{-26}$. Measurements of atmospheric neutrino flux by Super-Kamiokande [45] (round marker) and IceCube [46, 47] (triangle marker) for electron neutrinos (grey) and muon neutrinos (black). Predicted combined muon and electron neutrino atmospheric flux from Ref. [48] (solid grey line) is also displayed. [Right] DM annihilation cross-sections for which the DS neutrino flux peak exceeds that of the atmospheric background for a selection of f_{SMDS} and $f_\nu = 1/3$. Line colors indicate where Super-Kamiokande (dark blue) and IceCube (green) have leading sensitivity. Steep DS collapse model (thick lines) and gradual DS collapse model (thin lines), consistent with JWST candidate events, are shown. We assume DSs grow to 1% of their host halo mass in $M_h = 10^6 - 10^9 M_\odot$ halos, to an upper mass limit of $M_{\text{DS}} = 10^6 M_\odot$. Overlaid (shaded regions) are existing bounds from indirect DM detection searches in IceCube [49], Super-Kamiokande [50], and ANTARES [51]. The thermal relic DM annihilation cross-section [41] (gray dashed line) is displayed for reference.

events with neutrino energies determined by supernova temperatures, DSs emit neutrinos over prolonged time with neutrino energies determined by DM.

The electromagnetic comoving luminosity density of the total DS population as a function of redshift and integrated by DS age-distribution is

$$L_{\text{EM}}(z) = \int_0^{t(z)} d\tau \int_{M_{h,\text{min}}}^{M_{h,\text{max}}} dM_h L_{\text{DS}}(M_h, \tau) \times f_{\text{sur}}(z) \frac{d^2 n_{\text{DS}}}{dM_h dt}(M_h, z(t-\tau)), \quad (7)$$

where evaluating $d^2 n_{\text{DS}}/dM_h dt$ by differentiating Eq. (3) and evaluating at $z(t-\tau)$ gives the DS age τ distribution at cosmological time t formed in halos of mass M_h . Here, we do not include contributions from DM annihilation outside of DSs that is also enhanced by the adiabatic contraction, making our estimates conservative.

The resulting DS diffuse neutrino flux

$$\frac{d\phi}{dE_\nu} = \int_{z_{\text{lim}}}^\infty dz \left[(1+z) \frac{dN}{dE_\nu}(E_\nu(1+z)) \times \left(\frac{f_\nu}{(1-f_\nu)\langle E_\nu \rangle} L_{\text{EM}}(z) \right) \left| c \frac{dt}{dz} \right| \right] \quad (8)$$

where $\langle E_\nu \rangle$ is the average neutrino energy from DM annihilation and depends on considered channel (see

Supplemental Material), dN/dE_ν is a neutrino emission spectrum from DM annihilation and spectrum factor $(1+z)$ accounts for compression of the energy scale. In Ref. [43] $f_\nu = 1/3$ was assumed. For DM annihilation channels we consider neutrino spectra computed by Ref. [54, 55], summarized in Supplemental Materials. Here, $f_\nu/(1-f_\nu)\langle E_\nu \rangle$ converts the electromagnetic luminosity to neutrino number flux. We integrate from a minimum redshift where JWST becomes unable to observe the most massive DSs in our population $z_{\text{lim}} = 15$. In the Supplemental Material we show that our generalized formalism for extended source emission can also account for fluxes like DSNB.

Analysis results.— In Fig. 2 we display resulting DS neutrino flux at present for different DM annihilation channels and masses computed with Eq. (8), together with atmospheric neutrino background. We focus on signals when $E_\nu \gtrsim 200$ MeV. At lower energies contributions from solar, DSNB and reactor neutrinos also appears.

The DS neutrino flux has cut-off energy spectrum within factor of few of $E_\nu \sim m_\chi/(z_{\text{lim}} + 1) \sim m_\chi/16$, set by the DM mass and considered annihilation channel as well as redshift effects. Hence, such neutrino flux could be distinguished with atmospheric neutrino background including by spectral shape, depending on uncertainties. Further, at higher energies muon neutrinos dominate atmospheric flux [46], while the DS neutrino flux can con-

tain all flavors. For lower DM masses we find Super-Kamiokande [45] data can place the strongest bounds, while data from IceCube [46, 47] for $m_\chi \gtrsim 10$ TeV.

In Fig. 2 (right panel) we show DM parameters for which neutrino flux peak from DSs is estimated to exceed the atmospheric neutrino background when DM annihilation has $f_\nu = 1/3$ to $\nu\bar{\nu}$ for energies $E_\nu \gtrsim 200$ MeV following Super-Kamiokande [45] measurements, well fit by predictions [48], and at higher energies IceCube [46, 47] data. For reference, we overlay existing indirect detection constraints on DM annihilation. These estimated limits are seen to improve at higher DM masses due to different power law scaling between atmospheric flux and DS flux and at lower masses where the atmospheric flux flattens. Further, sensitivity at smaller DM masses increases also due to increased luminosity as seen from Eq. (4). These results can be further refined with detailed statistical analysis that we leave for future work. We estimated that a χ^2 analysis considering available data and uncertainties on detected neutrino energies (e.g. from Super-Kamiokande [45]) can be expected to yield results within $\sim 1-2$ orders of magnitudes of our present simplified treatment. At lighter masses the DS neutrino events become degenerate with those of DSNB, although with distinct spectra. At larger DM cross-sections, the electromagnetic emission from DSs is also enhanced and can affect other constraints. In the Supplementary Material we discuss DM annihilation to W^+W^- , $b\bar{b}$, and $\mu^+\mu^-$.

Upcoming large scale neutrino telescopes such as the 187-kton water Cherenkov detector Hyper-Kamiokande [56], 40 kton liquid argon DUNE [57, 58] and 20 kton liquid scintillator JUNO [59] can probe DSs fueled by \sim GeV–TeV scale DM with enhanced sensitivity.

Conclusions.— DSs provide compelling candidates for the first stars and potential seeds for SMBHs. Considering their neutrino emission and neutrino experiments, we estimated the first constraints on supermassive DSs and the DM interactions powering them from Super-Kamiokande and IceCube data, opening a novel window into SMBH progenitors. Our results are less sensitive to assumptions about DS populations and masses compared to direct searches such as with telescopes like JWST, offering a complementary approach to probing DSs at high redshifts. Our work paves the way for future probes of the nature of high redshift objects with upcoming neutrino telescopes including Hyper-Kamiokande, DUNE and JUNO as well as bridges fields of neutrino astronomy, DM physics, and early black hole formation.

Acknowledgments. We thank Katherine Freese, Tracy Slatyer, Anna Suliga and Tien-Tien Yu for discussions. V.T. acknowledges support by the World Premier International Research Center Initiative (WPI), MEXT, Japan and JSPS KAKENHI grant No. 23K13109. This work was performed in part at the Aspen Center for Physics, which is supported by the National Science

Foundation grant PHY-2210452.

* tschwem2@uoregon.edu

† vtakhist@post.kek.jp

- [1] T. Abel, G. L. Bryan, and M. L. Norman, *Science* **295**, 93 (2002), [arXiv:astro-ph/0112088](https://arxiv.org/abs/astro-ph/0112088).
- [2] V. Bromm, P. S. Coppi, and R. B. Larson, *Astrophys. J.* **564**, 23 (2002), [arXiv:astro-ph/0102503](https://arxiv.org/abs/astro-ph/0102503).
- [3] N. Yoshida, K. Omukai, L. Hernquist, and T. Abel, *Astrophys. J.* **652**, 6 (2006), [arXiv:astro-ph/0606106](https://arxiv.org/abs/astro-ph/0606106).
- [4] E. Vanzella, M. Meneghetti, G. B. Caminha, M. Castellano, F. Calura, P. Rosati, C. Grillo, M. Dijkstra, M. Gronke, E. Sani, A. Mercurio, P. Tozzi, M. Nonino, S. Cristiani, M. Mignoli, L. Pentericci, R. Gilli, T. Treu, K. Caputi, G. Cupani, A. Fontana, A. Grazian, and I. Balestra, *Monthly Notices of the Royal Astronomical Society* **494**, L81 (2020), [arXiv:2001.03619](https://arxiv.org/abs/2001.03619) [[astro-ph.GA](https://arxiv.org/abs/astro-ph.GA)].
- [5] B. Welch, D. Coe, J. M. Diego, A. Zitrin, E. Zackrisson, P. Dimauro, Y. Jiménez-Teja, P. Kelly, G. Mahler, M. Oguri, F. X. Timmes, R. Windhorst, M. Florian, S. E. de Mink, R. J. Avila, J. Anderson, L. Bradley, K. Sharon, A. Vikaeus, S. McCandliss, M. Bradač, J. Rigby, B. Frye, S. Toft, V. Strait, M. Trenti, S. Sharma, F. Andrade-Santos, and T. Broadhurst, *Nature (London)* **603**, 815 (2022), [arXiv:2209.14866](https://arxiv.org/abs/2209.14866) [[astro-ph.GA](https://arxiv.org/abs/astro-ph.GA)].
- [6] X. Wang, C. Cheng, J. Ge, X.-L. Meng, E. Daddi, H. Yan, Z. Ji, Y. Jin, T. Jones, M. A. Malkan, P. Arrabal Haro, G. Brammer, M. Oguri, M. Hou, and S. Zhang, *Astrophysical Journal Letters* **967**, L42 (2024), [arXiv:2212.04476](https://arxiv.org/abs/2212.04476) [[astro-ph.GA](https://arxiv.org/abs/astro-ph.GA)].
- [7] J. Matthee *et al.*, *Astrophys. J.* **963**, 129 (2024), [arXiv:2306.05448](https://arxiv.org/abs/2306.05448) [[astro-ph.GA](https://arxiv.org/abs/astro-ph.GA)].
- [8] M. Yue, A.-C. Eilers, R. A. Simcoe, R. Mackenzie, J. Matthee, D. Kashino, R. Bordoloi, S. J. Lilly, and R. P. Naidu, *The Astrophysical Journal* **966**, 176 (2024).
- [9] X. Ding, M. Onoue, J. D. Silverman, Y. Matsuoka, T. Izumi, M. A. Strauss, K. Jahnke, C. L. Phillips, J. Li, M. Volonteri, Z. Haiman, I. T. Andika, K. Aoki, S. Baba, R. Bieri, S. E. I. Bosman, C. Bottrell, A.-C. Eilers, S. Fujimoto, M. Habouzit, M. Imanishi, K. Inayoshi, K. Iwasawa, N. Kashikawa, T. Kawaguchi, K. Kohno, C.-H. Lee, A. Lupi, J. Lyu, T. Nagao, R. Overzier, J.-T. Schindler, M. Schramm, K. Shimasaku, Y. Toba, B. Trakhtenbrot, M. Trebitsch, T. Treu, H. Umehata, B. P. Venemans, M. Vestergaard, F. Walter, F. Wang, and J. Yang, *Nature (London)* **621**, 51 (2023), [arXiv:2211.14329](https://arxiv.org/abs/2211.14329) [[astro-ph.GA](https://arxiv.org/abs/astro-ph.GA)].
- [10] M. A. Stone, J. Lyu, G. H. Rieke, S. Alberts, and K. N. Hainline, *Astrophys. J.* **964**, 90 (2024), [arXiv:2310.18395](https://arxiv.org/abs/2310.18395) [[astro-ph.GA](https://arxiv.org/abs/astro-ph.GA)].
- [11] A. Bogdan *et al.*, *Nature Astron.* **8**, 126 (2024), [arXiv:2305.15458](https://arxiv.org/abs/2305.15458) [[astro-ph.GA](https://arxiv.org/abs/astro-ph.GA)].
- [12] B. P. Venemans, J. R. Findlay, W. J. Sutherland, G. De Rosa, R. G. McMahon, R. Simcoe, E. A. Gonzalez-Solares, K. Kuijken, and J. R. Lewis, *Astrophys. J.* **779**, 24 (2013), [arXiv:1311.3666](https://arxiv.org/abs/1311.3666) [[astro-ph.CO](https://arxiv.org/abs/astro-ph.CO)].
- [13] E. Banados *et al.*, *Nature* **553**, 473 (2018), [arXiv:1712.01860](https://arxiv.org/abs/1712.01860) [[astro-ph.GA](https://arxiv.org/abs/astro-ph.GA)].
- [14] M. Volonteri, *Astron. Astrophys. Rev.* **18**, 279 (2010),

- arXiv:1003.4404 [astro-ph.CO].
- [15] K. Inayoshi, E. Visbal, and Z. Haiman, *Ann. Rev. Astron. Astrophys.* **58**, 27 (2020), arXiv:1911.05791 [astro-ph.GA].
- [16] D. Spolyar, K. Freese, and P. Gondolo, *Phys. Rev. Lett.* **100**, 051101 (2008), arXiv:0705.0521 [astro-ph].
- [17] K. Freese, P. Bodenheimer, D. Spolyar, and P. Gondolo, *Astrophys. J. Lett.* **685**, L101 (2008), arXiv:0806.0617 [astro-ph].
- [18] D. Spolyar, P. Bodenheimer, K. Freese, and P. Gondolo, *Astrophys. J.* **705**, 1031 (2009), arXiv:0903.3070 [astro-ph.CO].
- [19] Y. Wu, S. Baum, K. Freese, L. Visinelli, and H.-B. Yu, *Phys. Rev. D* **106**, 043028 (2022), arXiv:2205.10904 [hep-ph].
- [20] J. C. Tan, J. Singh, V. Cammelli, M. Sanati, M. Petkova, D. Nandal, and P. Monaco, “The origin of super-massive black holes from pop iii.1 seeds,” (2024), arXiv:2412.01828 [astro-ph.GA].
- [21] D. R. G. Schleicher, R. Banerjee, and R. S. Klessen, *Phys. Rev. D* **79**, 043510 (2009), arXiv:0809.1519 [astro-ph].
- [22] A. Maurer, M. Raue, T. Kneiske, D. Horns, D. Elsasser, and P. H. Hauschildt, *Astrophys. J.* **745**, 166 (2012), arXiv:1201.1305 [astro-ph.CO].
- [23] Q. Yuan, B. Yue, B. Zhang, and X. Chen, *JCAP* **04**, 020 (2011), arXiv:1104.1233 [astro-ph.CO].
- [24] C. Ilie, J. Paulin, and K. Freese, *Proc. Nat. Acad. Sci.* **120**, e2305762120 (2023), arXiv:2304.01173 [astro-ph.CO].
- [25] F. Iocco, *Astrophys. J. Lett.* **677**, L1 (2008), arXiv:0802.0941 [astro-ph].
- [26] X.-D. Shi and G. M. Fuller, *Astrophys. J.* **503**, 307 (1998), arXiv:astro-ph/9801106.
- [27] X.-D. Shi, G. M. Fuller, and F. Halzen, *Phys. Rev. Lett.* **81**, 5722 (1998), arXiv:astro-ph/9805242.
- [28] F. Linke, J. A. Font, H.-T. Janka, E. Muller, and P. Papadopoulos, *Astron. Astrophys.* **376**, 568 (2001), arXiv:astro-ph/0103144.
- [29] V. Munoz, V. Takhistov, S. J. Witte, and G. M. Fuller, *JCAP* **11**, 020 (2021), arXiv:2102.00885 [astro-ph.HE].
- [30] D. Huterer, *The Astronomy and Astrophysics Review* **31**, 2 (2023).
- [31] S. M. Carroll, W. H. Press, and E. L. Turner, *Annual Review of Astronomy and Astrophysics* **30**, 499 (1992).
- [32] N. Aghanim *et al.* (Planck), *Astron. Astrophys.* **641**, A6 (2020), [Erratum: *Astron. Astrophys.* 652, C4 (2021)], arXiv:1807.06209 [astro-ph.CO].
- [33] W. H. Press and P. Schechter, *Astrophys. J.* **187**, 425 (1974).
- [34] R. K. Sheth and G. Tormen, *Mon. Not. Roy. Astron. Soc.* **308**, 119 (1999), arXiv:astro-ph/9901122.
- [35] E. Pierpaoli, D. Scott, and M. J. White, *Mon. Not. Roy. Astron. Soc.* **325**, 77 (2001), arXiv:astro-ph/0010039.
- [36] J. M. Bardeen, J. R. Bond, N. Kaiser, and A. S. Szalay, *Astrophys. J.* **304**, 15 (1986).
- [37] T. Rindler-Daller, M. H. Montgomery, K. Freese, D. E. Winget, and B. Paxton, *Astrophys. J.* **799**, 210 (2015), arXiv:1408.2082 [astro-ph.CO].
- [38] C. Ilie, K. Freese, M. Valluri, I. T. Iliev, and P. R. Shapiro, *Monthly Notices of the Royal Astronomical Society* **422**, 2164 (2012), eprint: <https://academic.oup.com/mnras/article-pdf/422/3/2164/18454337/mnras0422-2164.pdf>.
- [39] K. Freese, C. Ilie, D. Spolyar, M. Valluri, and P. Bodenheimer, *The Astrophysical Journal* **716**, 1397 (2010).
- [40] G. R. Blumenthal, S. M. Faber, R. Flores, and J. R. Primack, *Astrophys. J.* **301**, 27 (1986).
- [41] G. Steigman, B. Dasgupta, and J. F. Beacom, *Phys. Rev. D* **86**, 023506 (2012).
- [42] K. Freese, T. Rindler-Daller, D. Spolyar, and M. Valluri, *Rept. Prog. Phys.* **79**, 066902 (2016), arXiv:1501.02394 [astro-ph.CO].
- [43] K. Freese, T. Rindler-Daller, D. Spolyar, and M. Valluri, *Reports on Progress in Physics* **79**, 066902 (2016).
- [44] E. Zackrisson, P. Scott, C.-E. Rydberg, F. Iocco, B. Edvardsson, G. Östlin, S. Sivertsson, A. Zitrin, T. Broadhurst, and P. Gondolo, *Astrophys. J.* **717**, 257 (2010), arXiv:1002.3368 [astro-ph.CO].
- [45] E. Richard *et al.* (Super-Kamiokande), *Phys. Rev. D* **94**, 052001 (2016), arXiv:1510.08127 [hep-ex].
- [46] M. G. Aartsen *et al.* (IceCube), *Phys. Rev. D* **91**, 122004 (2015), arXiv:1504.03753 [astro-ph.HE].
- [47] M. G. Aartsen *et al.* (IceCube), *Astrophys. J.* **833**, 3 (2016), arXiv:1607.08006 [astro-ph.HE].
- [48] M. Honda, T. Kajita, K. Kasahara, and S. Midorikawa, *Phys. Rev. D* **83**, 123001 (2011), arXiv:1102.2688 [astro-ph.HE].
- [49] R. Abbasi *et al.* (IceCube), *Phys. Rev. D* **108**, 102004 (2023), arXiv:2303.13663 [astro-ph.HE].
- [50] K. Abe *et al.* (Super-Kamiokande), *Phys. Rev. D* **102**, 072002 (2020), arXiv:2005.05109 [hep-ex].
- [51] S. R. Gozzini (ANTARES, KM3NeT), *JINST* **16**, C09006 (2021).
- [52] M. J. Rieke *et al.*, *Astrophys. J. Suppl.* **269**, 16 (2023), arXiv:2306.02466 [astro-ph.GA].
- [53] E. W. Kolb, *The Early Universe*, Vol. 69 (Taylor and Francis, 2019).
- [54] M. Cirelli, G. Corcella, A. Hektor, G. Hütsi, M. Kadastik, P. Panci, M. Raidal, F. Sala, and A. Strumia, *Journal of Cosmology and Astroparticle Physics* **2011**, 051 (2011).
- [55] P. Ciafaloni, D. Comelli, A. Riotto, F. Sala, A. Strumia, and A. Urbano, *Journal of Cosmology and Astroparticle Physics* **2011**, 019 (2011).
- [56] K. Abe *et al.* (Hyper-Kamiokande), “Hyper-Kamiokande Design Report,” (2018), arXiv:1805.04163 [physics.ins-det].
- [57] B. Abi *et al.* (DUNE), *JINST* **15**, T08008 (2020), arXiv:2002.02967 [physics.ins-det].
- [58] R. Acciarri *et al.* (DUNE), “Long-Baseline Neutrino Facility (LBNF) and Deep Underground Neutrino Experiment (DUNE): Conceptual Design Report, Volume 2: The Physics Program for DUNE at LBNF,” (2015), arXiv:1512.06148 [physics.ins-det].
- [59] A. Abusleme *et al.* (JUNO), *Prog. Part. Nucl. Phys.* **123**, 103927 (2022), arXiv:2104.02565 [hep-ex].
- [60] K. Freese, P. Bodenheimer, D. Spolyar, and P. Gondolo, *The Astrophysical Journal* **685**, L101 (2008).
- [61] P. A. R. Ade *et al.* (Planck), *Astron. Astrophys.* **594**, A13 (2016), arXiv:1502.01589 [astro-ph.CO].
- [62] C. A. Iglesias and F. J. Rogers, *Astrophys. J.* **464**, 943 (1996).
- [63] J. F. Navarro, C. S. Frenk, and S. D. M. White, *Astrophys. J.* **490**, 493 (1997), arXiv:astro-ph/9611107.
- [64] M. Valluri, V. P. Debattista, T. Quinn, and B. Moore, *Monthly Notices of the Royal Astronomical Society* **403**, 525 (2010), eprint: <https://academic.oup.com/mnras/article->

pdf/403/1/525/3350458/mnras0403-0525.pdf.

- [65] K. Freese, D. Spolyar, and A. Aguirre, *Journal of Cosmology and Astroparticle Physics* **2008**, 014 (2008).
- [66] D. J. Eisenstein *et al.*, *arXiv e-prints*, arXiv:2306.02465 (2023), arXiv:2306.02465 [astro-ph.GA].
- [67] F. D’Eugenio, A. J. Cameron, J. Scholtz, S. Carniani, C. J. Willott, E. Curtis-Lake, A. J. Bunker, E. Parlanti, R. Maiolino, C. N. A. Willmer, P. Jakobsen, B. E. Robertson, B. D. Johnson, S. Tacchella, P. A. Cargile, T. Rawle, S. Arribas, J. Chevallard, M. Curti, E. Egami, D. J. Eisenstein, N. Kumari, T. J. Looser, M. J. Rieke, B. R. D. Pino, A. Saxena, H. Übler, G. Venturi, J. Witstok, W. M. Baker, R. Bhatawdekar, N. Bonaventura, K. Boyett, S. Charlot, A. L. Danhaive, K. N. Hainline, R. Hausen, J. M. Helton, X. Ji, Z. Ji, G. C. Jones, I. Joudžbalis, M. V. Maseda, P. G. Pérez-González, M. Perna, D. Puskás, I. Shivaeei, M. S. Silcock, C. Simmonds, R. Smit, F. Sun, N. C. Villanueva, C. C. Williams, and Y. Zhu, “Jades data release 3 – nirspec/msa spectroscopy for 4,000 galaxies in the goods fields,” (2024), arXiv:2404.06531 [astro-ph.GA].
- [68] J. F. Beacom, *Ann. Rev. Nucl. Part. Sci.* **60**, 439 (2010), arXiv:1004.3311 [astro-ph.HE].
- [69] C. A. Argüelles, A. Diaz, A. Kheirandish, A. Olivares-Del-Campo, I. Safa, and A. C. Vincent, *Rev. Mod. Phys.* **93**, 035007 (2021), arXiv:1912.09486 [hep-ph].
- [70] F. Prada, A. A. Klypin, A. J. Cuesta, J. E. Betancort-Rijo, and J. Primack, *Mon. Not. Roy. Astron. Soc.* **423**, 3018 (2012), arXiv:1104.5130 [astro-ph.CO].
- [71] L. Lopez-Honorez, O. Mena, S. Palomares-Ruiz, and A. C. Vincent, *JCAP* **07**, 046 (2013), arXiv:1303.5094 [astro-ph.CO].
- [72] K. Freese, P. Gondolo, J. A. Sellwood, and D. Spolyar, *Astrophys. J.* **693**, 1563 (2009), arXiv:0805.3540 [astro-ph].
- [73] D. R. G. Schleicher, R. Banerjee, and R. S. Klessner, *Phys. Rev. D* **78**, 083005 (2008), arXiv:0807.3802 [astro-ph].
- [74] A. Albert *et al.* (HAWC), *JCAP* **12**, 038 (2023), arXiv:2305.09861 [astro-ph.HE].
- [75] M. Ackermann *et al.* (Fermi-LAT), *Phys. Rev. Lett.* **115**, 231301 (2015), arXiv:1503.02641 [astro-ph.HE].
- [76] M. Aguilar *et al.* (AMS), *Phys. Rev. Lett.* **113**, 121102 (2014).
- [77] L. Accardo *et al.* (AMS), *Phys. Rev. Lett.* **113**, 121101 (2014).
- [78] H. Abdallah *et al.* (H.E.S.S.), *Phys. Rev. Lett.* **117**, 111301 (2016), arXiv:1607.08142 [astro-ph.HE].

SUPPLEMENTAL MATERIAL

Neutrino Whispers from Dark Stars Seeding Supermassive Black Holes

Thomas Schwemberger, Volodymyr Takhistov

Here, we provide additional details of DS evolution, population, computation of resulting diffuse neutrino flux as well as comparison to indirect DM detection.

DARK STAR MODEL AND EVOLUTION

We analytically investigate DS evolution by considering a polytrope model with hydrostatic and thermal equilibrium. This is expected to be in approximate agreement with detailed numerical evaluations of DS evolution with MESA 1D stellar evolution within a factor of few [37].

DSs are powered by DM heating instead of nuclear fusion in their cores and are of lower density and temperature than main sequence stars. With their equation of state typically dominated by non-relativistic gas pressure, DS stellar density profiles in early stages can be modeled as a polytrope with index $n = 3/2$ [60], describing systems supported primarily by thermal pressure with contributions from DM annihilation. In Ref. [18] later stages of DS evolution were modeled as $n = 3$ polytropes, considering dominance of radiation pressure. We confirmed that $n = 3$ polytropes result in larger DS volume and lower temperatures than their $n = 3/2$ counterparts, with resulting luminosity differing within a factor of few. Here, we use $n = 3/2$ throughout. The equation of state relating pressure P and density ρ is

$$P = K\rho^{1+1/n} , \quad (S1)$$

where n is the polytrope index and constant K is set by the stellar boundary conditions. We focus on $n = 3/2$ polytrope description of DSs.

For mass M_r contained within a radius r

$$M_r = \int_0^r dr' 4\pi r'^2 \rho(r') \quad (S2)$$

the hydrostatic equilibrium is

$$\frac{dP}{dr} = -\rho \frac{GM_r}{r^2} . \quad (S3)$$

Combining with Eq. (S1), this gives the well known Lane-Emden equation

$$\frac{1}{x^2} \frac{d}{dx} \left(x^2 \frac{d\theta}{dx} \right) = -\theta^n , \quad (S4)$$

in terms of the dimensionless variables $x = r/\alpha$, $\theta^n = \rho/\rho_c$ where $\alpha = (n+1)K/4\pi G\rho_c^{1-1/n}$ and ρ_c is the density at the center of the star. This is subject to the boundary conditions $\theta(0) = 1$, $d\theta/dx(0) = \theta'(0) = 0$, and $\theta(x_1) = 0$ where x_1 corresponds to the surface of the star. For $n = 3/2$, one finds $x_1 \simeq 3.65$. For a particular stellar radius R and mass M the constant K from Eq. (S1) is determined by

$$K = \frac{1}{n} \left[\left(\frac{R}{x_1} \right)^{-1+3/n} \left(\frac{GM}{-x_1^2 \theta'(x_1)} \right)^{1-1/n} (4\pi G)^{1/n} \right] . \quad (S5)$$

Here, we use the density contrast $D_n = \rho_c/\bar{\rho}$, which evaluates to $D_{3/2} = 5.99$ for $n = 3/2$, in order to set ρ_c .

We can then compute the photosphere radius R_s . The temperature is governed by the equation of state as

$$P(r) = \frac{\rho k_B T(r)}{\bar{m}} + \frac{4}{3} \frac{\sigma_B}{c} T(r)^4 , \quad (S6)$$

where σ_B the Stefan-Boltzmann constant, k_B is the Boltzmann constant, and $\bar{m} = m_u(2X+3Y/4)^{-1} \simeq 0.588m_u$ is the mean atomic weight in terms of mean atomic mass unit $m_u \simeq 0.931$ GeV with H and He mass fractions $X = 0.76$ and

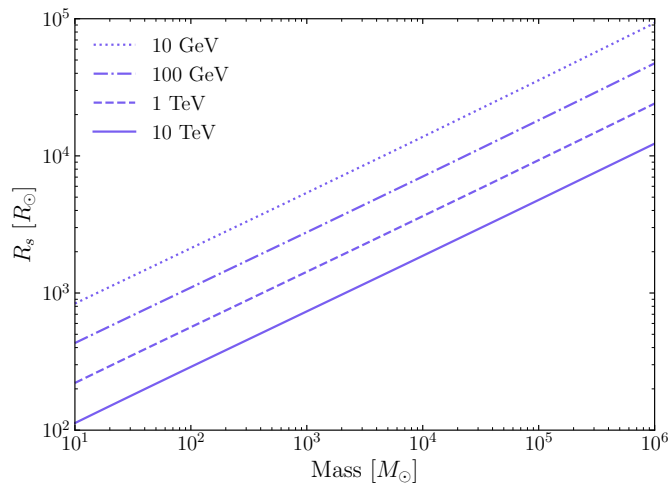


FIG. S1. DS photosphere radius for DM annihilation channel $\nu\bar{\nu}$ for different masses considering that the fraction of DM mass m_χ converted to neutrino energy is $f_\nu = 1/3$.

$Y = 0.24$, respectively, taken from Big Bang nucleosynthesis [61]. The resulting photosphere radius can be obtained by solving

$$P\kappa(\rho_{R_s}, T_{R_s}) = \frac{2}{3}g(R_s), \quad (\text{S7})$$

where κ is the opacity taken from numerically computed OPAL astrophysical opacity tables [62] and $g(r) = GM_r/r^2$ is the gravitational acceleration. Here, $\rho(r)$ is determined from the Lane-Emden equation (S4), P from the polytrope equation (S1), and T from the equation of state (S6). The surface luminosity is then determined from the obtained photosphere radius and effective temperature considered to be $T(R_s)$

$$L_{\text{surf}} = 4\pi\sigma_B R_s^2 T(R_s)^4. \quad (\text{S8})$$

We consider three distinct DS sources of energy playing a relevant role: (A) nuclear fusion, (B) gravitational energy and (C) DM heating via annihilation. Besides contributions from initial DM density, DM heating can benefit from the capture of additional DM from scattering with baryons in the star. We do not consider this contribution as it relies on additional assumptions about the DM-baryon interactions. Once DM is depleted, the star contracts and transitions to hydrogen burning. Prior to this, DM contributions dominate due to the lower core densities and pressures that suppress nuclear fusion, and the efficiency of DM annihilation. As DM annihilation products are converted into heat and heating the star more efficiently than fusion, neutrinos escape [16]. Therefore, we have

$$L_{\text{tot}} = L_{\text{fus}} + L_{\text{grav}} + L_{\text{DM}} \simeq L_{\text{DM}}. \quad (\text{S9})$$

The DM luminosity can be found from

$$L_{\text{DM}} \simeq (1 - f_\nu) \int_0^R dr 4\pi r^2 \frac{\langle\sigma v\rangle \rho_\chi^2}{m_\chi}. \quad (\text{S10})$$

Note that eq. (S10) is enhanced by a factor of two for Majorana particle DM. From Navarro-Frenk-White (NFW) DM profile [63] simulations, after adiabatic contraction the DM density at the outer edge of baryonic core is found to be [16]

$$\rho_\chi \simeq 1.7 \times 10^{11} \text{ GeV cm}^{-3} \left(\frac{n_b}{10^{13} \text{ cm}^{-3}} \right)^{0.81}, \quad (\text{S11})$$

where n_b is the baryon number density. We consider $n_b = 10^{13} \text{ cm}^{-3}$ at the initial DS formation, as in Ref. [16]. We then iteratively solve the polytrope equations. As a DS evolves, n_b changes accordingly. Outside the core, the DM is found to scale with $r^{-1.9}$. We adopt this as the representative DM density.

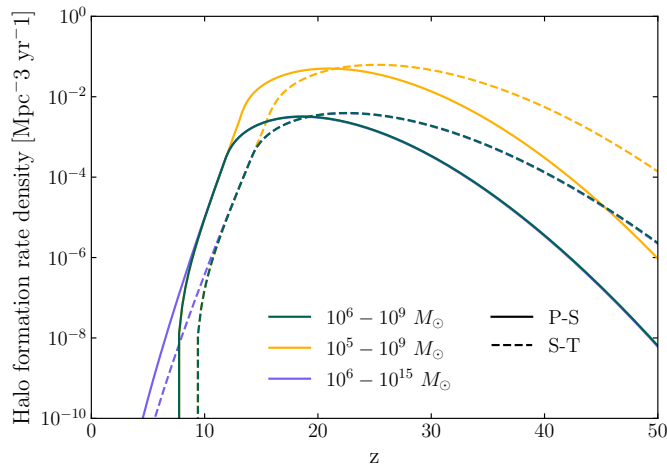


FIG. S2. Halo formation rate density $d^2n/dM_h dt$ integrated over halo mass range. Integrated halo formation rate density we consider as reference (green line), results extended to lighter halos (yellow line), results extended to more massive halos (lavender line) are shown. Press-Schechter (solid lines, P-S) and Sheth-Tormen (dashed lines, S-T) halo formation are indicated.

In thermal equilibrium, the luminosity of Eq. (S10) must balance the surface luminosity of Eq. (S8), with

$$L_{\text{DM,eq.}} = L_{\text{surf,eq.}} \quad (\text{S12})$$

In Fig. S1 we display the equilibrium radius as a function of time for DM annihilating to $\nu\bar{\nu}$ in a DS that reaches $10^6 M_\odot$ after prolonged accretion at $\dot{M} = 0.1 M_\odot \text{ yr}^{-1}$. To compute this, we first consider an initial DS radius value and find its photosphere radius. We then compare the surface and DM luminosities. After this, we iteratively adjust our initial radius as needed until Eq. (S12) is satisfied. This procedure yields resulting DS luminosity and radius as well as temperature, density, and pressure profiles for a given DS mass and DM particle mass. We have verified that for other DM decay channels results are similar.

Incorporating numerical simulations, analysis of Ref. [39] revealed that centrophilic orbits [64], which repeatedly pass through the star, can sustain the DM fuel supply for $\gtrsim 1$ Gyr. This extended fueling allows to support supermassive DSs, with their masses reaching $\gtrsim 10^6 M_\odot$ and luminosities of $10^9 - 10^{10} L_\odot$. In our study we also neglect the possibility of DM capture via scattering off baryons in DSs, which could extend their lifetime after the ambient DM density decreases. The effectiveness of this mechanism depends on the DM interactions with SM. The impact of DM capture on dark stars was initially studied in Ref. [65] and further refined in Ref. [43], where it was shown that stars fueled by captured DM are typically few times hotter and have radii smaller by an order of magnitude compared to those powered solely by adiabatic contraction.

Our results for supermassive DSs in Fig. 1 give luminosities that are approximately consistent with discussion of Ref. [37] indicating that luminosities obtained from polytropic model are expected to be suppressed by a factor of few compared to results from detailed stellar evolution simulations. We find that the DS luminosity can be well approximated by Eq. (4).

DARK STAR POPULATION AND COLLAPSE RATE

The halo density formation rate per halo mass $d^2n/dM_h dt$ can be obtained by differentiating Eq. (1) with respect to time. Integrated contributions over halo masses of the halo density formation rate in the total DS luminosity as described by Eq. (7) depend on the considered halo mass limits $M_{h,\text{min}}$ and $M_{h,\text{max}}$. In Fig. S2 we illustrate the effect of different choices of the halo mass limits on the integral of $d^2n/dM_h dt$ with respect to M_h . Increasing $M_{h,\text{max}}$ does not have an appreciable effect at z_{lim} since massive halos become increasingly rare at higher redshifts. On the other hand, decreasing $M_{h,\text{min}}$ substantially increases the halo density formation rate due to larger contributing population of smaller halos. These lighter halos are less luminous and thus result in a smaller enhancement on the flux despite being numerous.

As discussed in the main text, DSs can potentially be detected by sensitive telescopes such as JWST. For $10^6 M_\odot$ DSs, with luminosities of $10^{10} L_\odot$, we consider that JWST can observe all such objects that survive beyond $z = 15$.

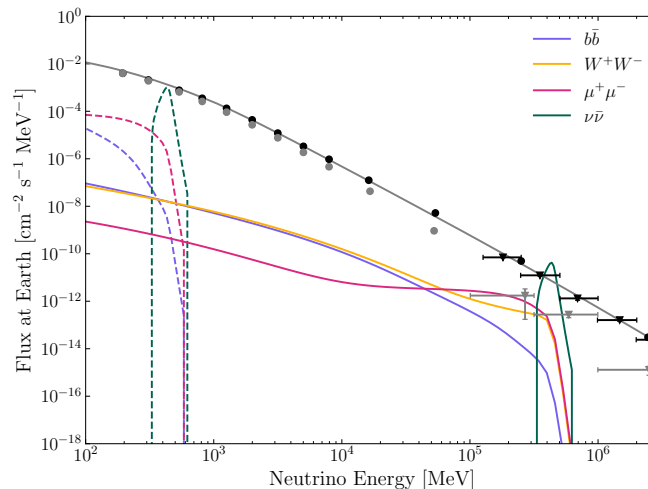


FIG. S3. Same as Fig. 2 considering gradual DS collapse model with f_{sur} given by Eq. (S14).

Three DS candidates have been identified considering JWST JADES survey [24], which initially covered approximately $\sim 26.4 \text{ arcmin}^2$ [52, 66]. Since the identification of these candidates, the JADES survey has expanded its observational area to $\sim 56 \text{ arcmin}^2$ [67]. We assume JWST can efficiently identify such DSs. Then, to remain consistent with these observations, the majority of $\sim 10^6 M_{\odot}$ DSs should collapse before $z = 15$.

In our analysis, we model DS collapse with a step function in redshift

$$f_{\text{sur}} = 1 - \Theta(z - z_{\text{lim}}) \quad (\text{S13})$$

where Θ is the Heaviside step function. We also consider a more gradual collapse scenario, with a DS survival fraction parameterized by

$$f_{\text{sur}} = \frac{1}{2} \left[1 + \tanh(z - z_0) \right], \quad (\text{S14})$$

where z_0 is a redshift parameter. In the framework of Eq. (S14), a fraction of the population survives to later times. Observations by JWST allow to constrain the surviving DS fraction and combination $f_{\text{SMDS}} f_{\text{sur}}$. Choosing $f_{\text{SMDS}} = 10^{-2}$ as a reference values, consideration of $z_0 \simeq 22$ allows for three candidate objects in the 26.4 arcmin^2 JADES field of view as claimed by analysis of Ref. [24]. Additional data from JWST will expand the angular coverage θ^2 . If no additional DS candidates are found, the resulting constraints on the population of luminous DSs will become more strict. Specifically, the bounds on the number of detectable DSs at high luminosities can be improved, with results scaling as $\propto N/\theta^2$ (see Eq. (5)). Our approach establishes a direct connection between DS diffuse neutrino emission and the DS candidates of JWST.

In Fig. S3, we display the predicted DS neutrino flux considering gradual DS collapse with f_{sur} following Eq. (S14) and compare with Fig. 2 based on step function rapid DS collapse model of Eq. (S13). The gradual DS collapse model gives neutrino flux predictions suppressed by around an order of magnitude compared to the step-function model. This originates from constraints on the low-redshift tail of the DS population that also impact DS population at higher redshifts.

GENERALIZED DIFFUSE NEUTRINO FLUX

Our general formalism of Eq. (8), and considering Eq. (7) as the comoving luminosity density of population of sources, captures extended source emission with variety of source lifetimes. This can readily reduce to conventional formalism for transient sources [68]. In particular, we can consider the DSNB with evolving redshift-dependent core-collapse supernova rate $R_{\text{SN}}(z)$.

Let us consider DS luminosity as a Dirac delta function

$$L_{\delta} = L_0 \delta(\tau), \quad (\text{S15})$$

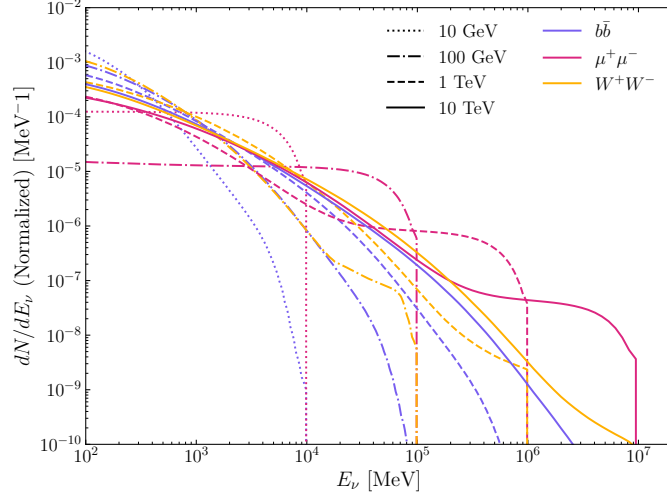


FIG. S4. Differential neutrino spectra normalized to one neutrino for a range of DM masses from $m_\chi = 10$ GeV to 10 TeV for different DM annihilation channels. Spectra are taken from Ref. [54, 55]

Annihilation channel	$m_\chi = 10$ GeV		$m_\chi = 100$ GeV		$m_\chi = 10$ TeV		$m_\chi = 100$ TeV	
	f_ν	$\langle E_\nu \rangle$ (GeV)	f_ν	$\langle E_\nu \rangle$ (GeV)	f_ν	$\langle E_\nu \rangle$ (GeV)	f_ν	$\langle E_\nu \rangle$ (GeV)
bb	0.47	0.224	0.45	0.944	0.45	4.19	0.45	19.8
$\mu^+\mu^-$	0.63	3.13	0.62	31.0	0.62	206	0.61	1113
W^+W^-	N/A	N/A	0.50	1.28	0.52	9.32	0.50	46.3
$\nu\bar{\nu}$	1/3	10	1/3	100	1/3	10^3	1/3	10^4

TABLE S1. Fraction f_ν of DM mass m_χ emitted as neutrino energy different DM masses and annihilation channels. The $\nu\bar{\nu}$ channel only produces neutrinos and hence does not inherently allow powering DSs through heating when $f_\nu = 1$, and we consider $f_\nu \sim 1/3$.

with $L_0 = \int d\tau L_{DS}(\tau)$ such that the total integrated DS luminosity is identical to that of prolonged emission. Note that Eq. (S15) also implies all DS emission occurs at formation, with $\tau = 0$, allowing to neglect f_{sur} . With this luminosity, Eq. (7) becomes

$$\begin{aligned}
 L_{\text{EM}}(z) &= \int_0^{t(z)} d\tau \int_{M_{\text{min}}}^{M_{\text{max}}} dM_h L_0 \delta(\tau) \frac{d^2 n_{\text{DS}}}{dM_h dt} (z(t-\tau), M_h) \\
 &= L_0 \int_{M_{\text{min}}}^{M_{\text{max}}} dM_h \frac{d^2 n_{\text{DS}}}{dM_h dt} (z(t), M_h) = L_0 R(z).
 \end{aligned} \tag{S16}$$

where in Eq. (S16) we have identified $R(z)$ as the rate density of DS formation that is analogous to supernova rate $R_{\text{SN}}(z)$ in computation of DSNB [68].

From this computation, our Eq. (8) becomes Eq. (S17), where $L_0 f_\nu / (1 - f_\nu) \langle E_\nu \rangle$ is the number flux of neutrinos emitted per DS and spectrum dN/dE is normalized. Hence, $(dN/dE_\nu) L_0 f_\nu / (1 - f_\nu) \langle E_\nu \rangle$ is the neutrino emission from a single DS analogous to the DSNB emission spectrum ϕ in Ref. [68] in units of neutrinos per unit energy. Under these considerations, Eq. (S17) can be matched with DSNB flux computation of Ref. [68]

$$\frac{d\phi}{dE_\nu} = \int dz \left[(1+z) \frac{dN}{dE_\nu} (E_\nu(1+z)) \frac{f_\nu / (1 - f_\nu)}{\langle E_\nu \rangle} L_0 \right] [R(z)] \left| c \frac{dt}{dz} \right|. \tag{S17}$$

In Fig. S4 we show the neutrino spectra dN/dE obtained from Ref. [54] and list a selection of neutrino fractions in Tab. S1.

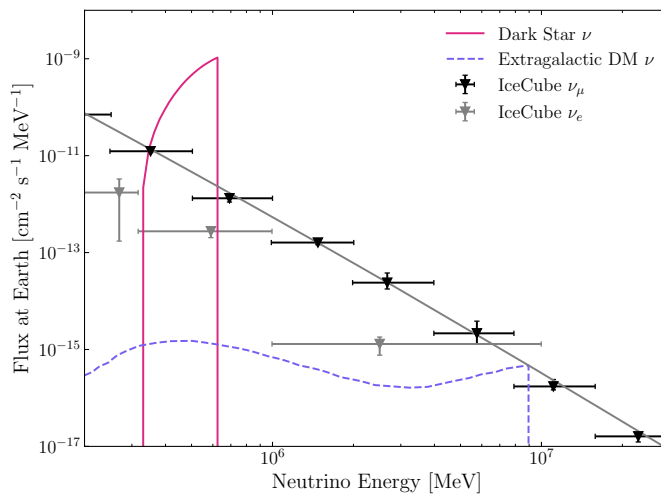


FIG. S5. Extragalactic neutrino flux from 10 TeV DM annihilating in dark stars (pink/solid) assuming DS reach 1% of their host halo mass which is in the range $M_h = 10^6 - 10^9 M_\odot$ compared to the expected neutrino flux from conventional dark matter halos (purple/dashed) from [69].

COMPARISON WITH INDIRECT DARK MATTER DETECTION

DM annihilation can produce a range of observable signatures, including extragalactic diffuse gamma-ray background and the diffuse neutrino background. Here we examine how the emission from DSs associated with DM annihilation compares to signals in the context of indirect DM detection.

Since DM annihilation follows $\propto \rho_{\text{DM}}^2$ for DM density ρ_{DM} , we define f_{DS} as the enhancement factor representing the overdensity of DM annihilation within DS compared to that in a typical galactic DM profile, which we assume follows the NFW [63] distribution

$$f_{\text{DS}} = \frac{\int_0^{r_{\text{DS}}} \rho_{\text{DS}}^2(r) r^2 dr}{\int_0^{r_\Delta} \rho_h^2(r) r^2 dr}. \quad (\text{S18})$$

Here, ρ_{DS} is the DS density profile, r_{DS} is the DS radius and ρ_{NFW} is the NFW profile density

$$\rho_h = \frac{4\rho_s}{(r/r_s)(1+r/r_s)^2} \quad (\text{S19})$$

where r_s is the characteristic radius and ρ_s is the characteristic density.

We consider r_Δ to denote the outer radius of the halo such that

$$M_h = \Delta \rho_c(z) \frac{4}{3} \pi r_\Delta^3, \quad (\text{S20})$$

where $\rho_c(z) \simeq \rho_c(\Omega_m(1+z)^3 + \Omega_\Lambda)$ is the critical density of the Universe with Ω_m and Ω_Λ denoting fractional contributions from matter and dark energy [32]. Hence, the density within r_Δ is Δ times the critical density of the Universe. Following Ref. [70], we consider overdensity threshold $\Delta = 200$. Then, the halo concentration is found from $c_\Delta = r_\Delta/r_s$. We employ $c_\Delta(M_h, z)$ parametrization of Ref. [71] obtained from the fit of all available data from the MultiDark/BigBolshoi simulations [70], and which enters as

$$\int_0^{r_\Delta} \rho_h^2(r) r^2 dr = \tilde{g}(c_\Delta) \frac{M_h \Delta \rho_c(z)}{12\pi} \quad (\text{S21})$$

where \tilde{g} is given by

$$\tilde{g}(c_\Delta) = \frac{c_\Delta^3 [1 - (1 + c_\Delta)^{-3}]}{3[\ln(1 + c_\Delta) - c_\Delta/(1 + c_\Delta)]^2}. \quad (\text{S22})$$

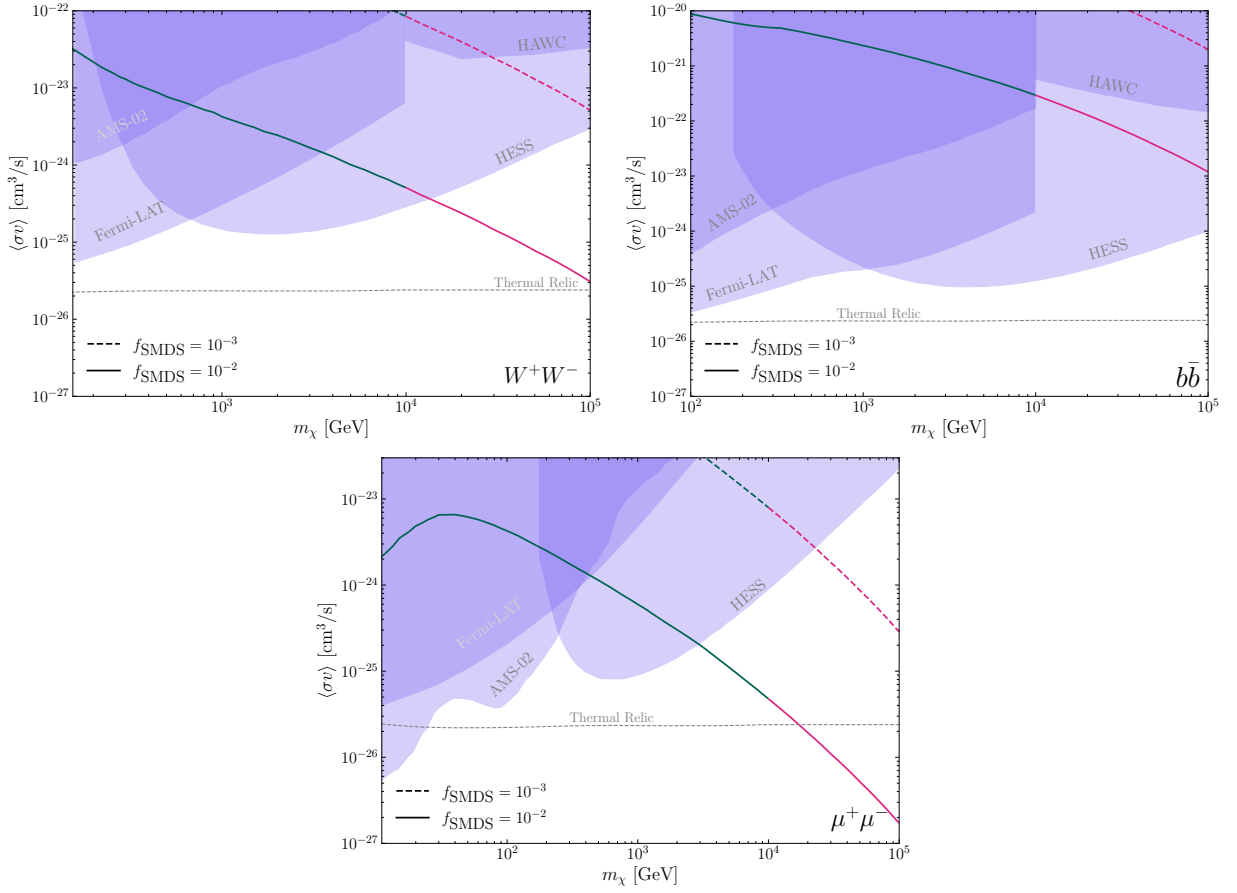


FIG. S6. Same as Fig. 2, but for DM annihilation to W^+W^- [Top Left], $b\bar{b}$ [Top Right] and $\mu^+\mu^-$ [Bottom]. Existing bounds from indirect DM detection searches by HAWC [74], Fermi-LAT [75], AMS [76, 77] and HESS [78] are shown as shaded regions.

Previously, analysis of DS gamma-ray background of Ref. [23] found that DM annihilation rate from DSs exceeds that of halos by enhancement of $f_{\text{DS}} \sim 10^3$. They considered DS density profiles of Ref. [72] for $\sim 10 - 100 M_\odot$ DS forming in a $10^5 - 10^6 M_\odot$ halo. Using of Ref. [72] we have computed similar $f_{\text{DS}} \sim 10^3$ to that of Ref. [23]. Importantly, those profiles correspond to very early phase in DS formation when baryonic matter has only contracted to a hydrogen density of $\sim 10^{13} \text{cm}^{-3}$.

However, as can be seen from Ref. [37] for the supermassive DSs we consider, the baryon densities reach nearly $\sim 10^{20} \text{cm}^{-3}$. For an increase in density from 10^{13}cm^{-3} to 10^{16}cm^{-3} , considering the DS and halo mass is the same and DS mass is only $M_{\text{DS}} \sim 10^{-4} M_h$, the enhancement factor significantly increases to $f_{\text{DS}} \sim 10^6$. For supermassive DSs we study, as DSs further evolve and grow to $\sim 1\%$ of the halo mass the enhancement factor increases to $f_{\text{DS}} \sim 10^8$. For a $M_h = 10^8 M_\odot$ halo we find $f_{\text{DS}} = 4 \times 10^8$ for a DS of mass $M_{\text{DS}} = 10^6$.

As we have demonstrated, supermassive DSs we explore benefit from greater enhancements f_{DS} compared to what was found in earlier studies (e.g. [23]) that focused on less concentrated smaller and earlier DSs that compose a less significant fraction of the host halo mass. We note that constraints from the extragalactic diffuse gamma-ray background have not been evaluated in such case in detail, which we leave for future work. We note that DS electromagnetic radiation has also been studied in the context of reionization [21, 73], however these analyses relied on a DS phases after DM depletion.

Besides electromagnetic diffuse emission, we can also compare DS emission with halo emission for DM annihilating to neutrinos. For comparison to the extragalactic neutrino flux from indirect DM detection, we are now interested in contributions from the entire halo population and compare to results of Ref. [69]. Noting that f_{DS} varies by only $\mathcal{O}(1)$ factors for halo masses in the range of $10^6 M_\odot$ to $10^9 M_\odot$, we assume a constant value $f_{\text{DS}} \simeq 10^8$ for DSs that reach 1% of the halo mass. Since only massive halos in the range $10^6 - 10^9 M_\odot$ can host supermassive DSs, this enhancement is suppressed. Halos less than $10^6 M_\odot$ are far more abundant and we find that they contribute $\sim 10^3$ times more to the extragalactic neutrino flux than the heavier portion of the halo population. Thus $f_{\text{DS}} \sim 10^8$ enhances only

portion of the total diffuse DS neutrino flux that is suppressed by a $\sim 10^{-3}$ due to subdominant contributions of large halos hosting DSs. From these approximate considerations, we expect supermassive DSs to enhance the neutrino flux compared to DM annihilation by a factor $\sim 10^5$. In Fig. S5 we display our computational results, showing qualitative agreement with the estimates above and finding that the DS neutrino flux exceeds that of halos by around $\sim 10^6$.

DIFFERENT DARK MATTER ANNIHILATION CHANNELS

In the main text we focused on results for DM annihilating to $\nu\bar{\nu}$. In Fig. S6 we provide results for DM annihilation to W^+W^- , $b\bar{b}$ and $\mu^+\mu^-$ channels. As in Fig. 2 of the main text, we show DM annihilation cross-sections for which neutrino emission from DSs in a fraction f_{SMDS} of halos exceeds the atmospheric background at energies $E_\nu \gtrsim 200$ MeV. The total energy radiated in neutrinos is primarily determined by DS luminosity, which only weakly depends on DM annihilation channel. The difference in these results stems from the different neutrino spectra, with softer spectra such as that of $b\bar{b}$ channel being more challenging to distinguish and identify than the peaked spectra such as from $\nu\bar{\nu}$ channel.